Journal of Computational Mathematics, Vol.24, No.3, 2006, 401–411.

MODEL ANALYSIS AND PARAMETER EXTRACTION FOR MOS CAPACITOR INCLUDING QUANTUM MECHANICAL EFFECTS *1)

Hai-yan Jiang Ping-wen Zhang
(*LMAM, CCSE and School of Mathematical Sciences, Peking University, Beijing 100871, China*)

Dedicated to the 70th birthday of Professor Lin Qun

Abstract

The high frequency CV curves of MOS capacitor have been studied. It is shown that semiclassical model is a good approximation to quantum model and approaches to classical model when the oxide layer is thick. This conclusion provides us an efficient (semiclassical) model including quantum mechanical effects to do parameter extraction for ultrathin oxide device. Here the effective extracting strategy is designed and numerical experiments demonstrate the validity of the strategy.

Mathematics subject classification: 81V10, 65M32.
Key words: Poisson Equation, Schrödinger Equation, MOS Capacitor, Quantum Effect, Sensitivity, Parameter Extraction.

1. Introduction

Metal-Oxide-Semiconductor (MOS) structure is the core of MOS technology. This structure becomes a capacitor with one side relating to the metal and the other side to semiconductor. Its capacity depends on the gate voltage. This structure is very important for the building technique of MOS integrated circuits. In fact CV(capacity and gate voltage) curve is often measured to estimate the performance of the integrated circuits. The important parameters, such as the thickness of the oxide layer, the doping profile of the substrate is determined by fitting CV curve. Due to the high nonlinearity of the mathematical model, it is difficult to obtain an analytical solution. So we have to resort to numerical method.

For large scale MOS structure, much work about the classical model has been described in [1, 12]. As MOS devices are scaled to deep sub-micro dimensions, aggressive scaling of gate dielectric thickness has continued. According to the National Technological Roadmap for semiconductor (NTRS) [2], the scaling trend for gate dielectrics is such that for sub-100 nm generation device, an equivalent gate oxide thickness of less than 3.0 nm will be required [10]. The combination of thin gate dielectrics and high level gate bias results in deep submicron ($< 0.25\mu m$) MOS device in large transverse electric fields at the interface. When the transverse electric fields become large enough to cause the formation of a 2-D electron (or hole) gas, the modelling of quantum mechanical (QM) effects in inversion and accumulation layers becomes very important. QM effects result in decreased inversion layer charge density in the inversion layer at a given gate voltage (compared to classical calculations which ignore QM effects) [5]. An accurate model should be the completely coupled Poisson equation and Schrödinger equation. The electrostatic potential and quantum energy levels of an accumulated n-type semiconductor is fully self-consistently calculated in [9]. According to physical characteristic, additional boundary condition is set to Poisson equation and shooting method is applied the initial problem. Schrödinger equation is solved by shifting energy to make sure the wave function

* Received March 1, 2006.
1) This work is partially supported by National Science Foundation of China for Distinguished Young Scholars 10225103 and 90207009.

not to distort physical properties in oxide layer. Finite difference method is used to solve Poisson and Schrödinger equations self-consistently for accumulated layers [7] and applied to the calculation of tunnelling current. The fully self-consistent QM treatment of the inversion layer and accumulation layer is time-consuming and too cumbersome for practical device simulation. To do parameter extraction for ultrathin oxide gate device, it is important to choose an efficient model including QM effects. QM effects is obvious only in the potential well at the interface of oxide layer and Si layer, so it is not necessary to include QM effect in the global region. In this paper, the semiclassical model is presented, quantum region is located at the beginning of the Si layer, which is set large enough to include QM effects and other regions are considered classically.

The main purpose of this paper is to analyze the different scale mathematical models and extract important parameters. The physical model and mathematical models are introduced in section 2. Numerical method is presented and which is used to identify the phenomena for different models in section 3. In section 4, inverse strategy is designed and inverse result is given. Finally, we draw the conclusion in section 5.

2. Physical and Mathematical Model of 1-D MOS Capacitor

1-D MOS capacitor consists of three layers: Poly-Si (metal), Sio_2 layer (oxide) and Si layer from the left to the right as shown in figure 1. QM effects are obvious at the beginning of the Si layer. As we mentioned in the previous section, our approach aims at self-consistently solving the Schrödinger and Poisson equations. Although the same procedure is applicable to any semiconductor-insulator combination, as an example of illustration, we shall consider the case of n-type Si/Sio_2/Poly-Si structure.

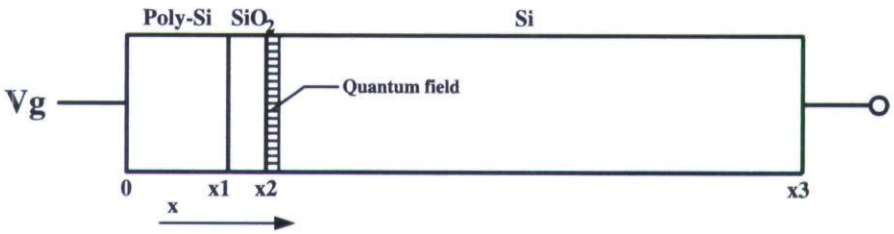

Figure 1: The structure of MOS capacitor

The following is a list of physical parameters to be used in our MOS capacitor model.

- k is Boltzman constant $\quad k = 1.38066 \times 10^{-23} J/K$
- $\hbar$ is Plank constant $\quad \hbar = 1.05457266 \times 10^{-34} J.s$
- m_0 is electron mass $\quad m_0 = 9.109 \times 10^{-31} kg$
- E_g is the length of band gap in Si $\quad E_g = 1.12ev$
- q is electron charge $\quad q = 1.60218 \times 10^{-19} C$
- T is room temperature $\quad T = 300K$
- Q_{it} is the interface-trapped charge density; $\quad Q_{it} = 3 \times 10^{10} cm^{-2}$
- n_i is intrinsic carrier concentration; $\quad n_i = 1.45 \times 10^{10} cm^{-3}$
- t_{poly} is thickness of Poly-Si layer $\quad t_{poly} = 0.01\mu m = 10nm$
- t_{si} are thickness of Si layers. $\quad t_{si} = 0.2\mu m = 200nm.$

2.1. Poisson Equation

Poisson Equation is the fundamental equation which governs the electrostatic potential and the charge distribution:

$$-\frac{\mathrm{d}}{\mathrm{d}x}\left(\varepsilon(x)\frac{\mathrm{d}\phi(x)}{\mathrm{d}x}\right) = \rho(\phi(x), x) = q(p(x) - n(x) + N_d(x)) \tag{1}$$

with the boundary conditions:

$$\begin{cases} \phi|_{x=0} = \phi_0 + \phi_{Bpoly} = \phi_0 + \dfrac{\mathrm{kT}}{\mathrm{q}} \ln\left(\dfrac{N_{0poly}}{\mathrm{n_i}}\right) \\ \phi|_{x=x_3} = \phi_B = \dfrac{\mathrm{kT}}{\mathrm{q}} \ln\left(\dfrac{N_{const}}{\mathrm{n_i}}\right), \end{cases} \tag{2}$$

where x is the depth from the left boundary of the device, $\phi(x)$ is the electrostatic potential at x, $\varepsilon(x)$ is the material's dielectric number and is a constant in three layers respectively. The effective gate potential ϕ_0 is the difference of the gate potential V_g and the flatten band potential V_{fb}: $\phi_0 = V_g - V_{fb}$. $\rho(x)$ is the total charge density composed of electron density $n(x)$, hole density $p(x)$ and doping density $N_d(x)$. In Poly-Si layer, the doping profile is approached as

$$N_{poly}(x) = N_{0poly}[1 - \exp(\frac{x - T_{poly}}{\sigma_1})].$$

In oxide layer, $N_d(x) = 0$. In Si layer, Gaussian function was selected to describe the doping profile [6]:

$$N_{si}(x) = N_{0si} \exp[-(\frac{x - x_0}{\sqrt{2}\sigma_2})^2] + N_{const}.$$

Different scale models have different charge density form [4]. With free charge approximation, classical model has the charge density:

$$\rho(\phi(x), x) = \begin{cases} \mathrm{q}\left[\mathrm{n_i} \exp\left(\dfrac{-\mathrm{q}(\phi(x) - \phi_0)}{\mathrm{kT}}\right) - \mathrm{n_i} \exp\left(\dfrac{\mathrm{q}(\phi(x) - \phi_0)}{\mathrm{kT}}\right) + N_{poly}(x)\right] & \text{in } Poly\text{-}Si \\ -\mathrm{Q_{it}}\delta(x_2) & \text{in } Sio_2 \\ \mathrm{q}\left[\mathrm{n_i} \exp\left(\dfrac{-\mathrm{q}\phi(x)}{\mathrm{kT}}\right) - \mathrm{n_i} \exp\left(\dfrac{\mathrm{q}\phi(x)}{\mathrm{kT}}\right) + N_{si}(x)\right] & \text{in } Si \text{ layer.} \end{cases} \tag{3}$$

As the device scale decreases, QM effects can not be ignored. To include QM effects, the coupled Poisson equation and Schrödinger equation must be solved self-consistently. Electrostatic potential $\phi(x)$ determines the potential function for Schrödinger equation while charge density function $\rho(x)$ is dependent on the solution of Schrödinger equation. In semiclassical model, it is assumed that charges are trapped in the potential well at the beginning of Si layer and the charge density of semiclassical model is:

$$\rho(\phi(x), x) = \begin{cases} \mathrm{q}\left[\mathrm{n_i} \exp\left(\dfrac{-\mathrm{q}(\phi(x) - \phi_0)}{\mathrm{kT}}\right) - \mathrm{n_i} \exp\left(\dfrac{\mathrm{q}(\phi(x) - \phi_0)}{\mathrm{kT}}\right) + N_{poly}(x)\right] & \text{in } Poly\text{-}Si \\ -\mathrm{Q_{it}}\delta(x_2) & \text{in } Sio_2 \\ \mathrm{q}\left[p_{qm}(x) - n_{qm}(x) + N_{si}(x)\right] & \text{in QM region} \\ \mathrm{q}\left[\mathrm{n_i} \exp\left(\dfrac{-\mathrm{q}\phi(x)}{\mathrm{kT}}\right) - \mathrm{n_i} \exp\left(\dfrac{\mathrm{q}\phi(x)}{\mathrm{kT}}\right) + N_{si}(x)\right] & \text{elsewhere in } Si. \end{cases} \tag{4}$$

In fact, electrons and holes possibly penetrate into the oxide layer. To describe the charge distribution correctly, it is necessary to include QM effects in the total Oxide layer and Si layer.

So the quantum model's charge density is:

$$\rho(\phi(x),x)=\begin{cases}\mathrm{q}\left[\mathrm{n_i}\exp\left(\dfrac{-\mathrm{q}(\phi(x)-\phi_0)}{\mathrm{kT}}\right)-\mathrm{n_i}\exp\left(\dfrac{\mathrm{q}(\phi(x)-\phi_0)}{\mathrm{kT}}\right)+N_{poly}(x)\right] & \text{in } Poly\text{-}Si\\ \mathrm{q}\left[p_{qm}(x)-n_{qm}(x)+N_d(x)\right] & \text{in } Sio_2 \text{ and Si}\end{cases} \tag{5}$$

$p_{qm}(x)$ and $n_{qm}(x)$ are the hole density and electron density of the quantum region with the index qm to denote quantum effect. Before $p_{qm}(x)$ and $n_{qm}(x)$ are computed, stationary Schrödinger equation must be considered.

2.2. Schrödinger Equation

For semiclassical model, it is assumed that the potential barrier at the interface of oxide layer and Si layer is infinite and charge are trapped in the narrow potential well. So it is reasonable to set zero boundary condition to Schrödinger equation at quantum region boundary:

$$\begin{cases}\left[-\dfrac{\hbar^2}{2m^*}\dfrac{\mathrm{d}^2}{\mathrm{d}x^2}+\mathrm{q}V^*(x)\right]\psi_j(x)=E_j\psi_j(x)\\ \psi_j(x_2)=0\\ \psi_j(x_2+L_q)=0\end{cases} \tag{6}$$

where L_q is the width of the quantum region. The barrier height is about 3.2ev for electrons and 4.8ev for holes at the interface of oxide layer and Si layer. Electrons and holes possibly penetrate into oxide layer [8]. Thus, wave functions should penetrate into oxide layer. Complete quantum model describes it correctly. The corresponding Schrödinger equation is:

$$\begin{cases}\left[-\dfrac{\hbar^2}{2m^*(x)}\dfrac{\mathrm{d}^2}{\mathrm{d}x^2}+\mathrm{q}V^*(x)\right]\psi_j(x)=E_j\psi_j(x)\\ \psi_j(x_1)=0\\ \psi_j(x_3)=0\end{cases} \tag{7}$$

The wave function and velocity are continuous at the interface of oxide layer and Si layer:

$$\psi(x_2^-)=\psi(x_2^+) \qquad \frac{1}{m_{ox}}\frac{\partial\psi(x_2^-)}{\partial x}=\frac{1}{m_{si}}\frac{\partial\psi(x_2^+)}{\partial x}.$$

m^* is the effective mass of charge and space dependent ($m_{ox}=0.5m_0$ in oxide layer). $V^*(x)$ is the potential function, linear dependent on static potential in oxide layer for quantum model. Index $*$ indicates different value of m^* and $V^*(x)$ according to different charge (hole or electron) and different degeneration in Si.
For electron,

$$V^*(x)=V_e(x)=\frac{E_g}{2\mathrm{q}}-(\phi(x)-\phi_B) \qquad V_e(x_2^-)=V_e(x_2^+)+3.2.$$

For Hole,

$$V^*(x)=V_h(x)=\frac{E_g}{2\mathrm{q}}+(\phi(x)-\phi_B) \qquad V_h(x_2^-)=V_h(x_2^+)+4.8.$$

The density state of 2-D electron (hole) gas is constant $N(E)=\dfrac{m}{\pi\hbar^2}$. Energy occupation is governed by the Fermi-Dirac distribution $f(E,E_F,T)$:

$$f(E,E_F,T)=[\exp(\frac{E-E_F}{kT})+1]^{-1}.$$

Thus, the density of charge per unit area is given by

$$n = \int N(E) f(E, E_F, T) dE.$$

After computing E_j and $\psi_j(x)$ and superposing different degenerations, $n_{qm}(x)$ and $p_{qm}(x)$ can be deduced [4]:

$$n_{qm}(x) = \frac{\mathrm{kT}}{\pi\hbar^2} \sum_{i=1}^{2} \mathrm{g_{e}}_i \mathrm{m_{eD}}_i \sum_j \ln\left[1 + \exp\left(\frac{-E_F - E_{eij}}{\mathrm{kT}}\right)\right] \left|\psi_{eij}(x)\right|^2, \tag{8}$$

$$p_{qm}(x) = \frac{\mathrm{kT}}{\pi\hbar^2} \sum_{i=1}^{3} \mathrm{g_{h}}_i \mathrm{m_{hD}}_i \sum_j \ln\left[1 + \exp\left(\frac{E_F - E_{\mathrm{h}ij}}{\mathrm{kT}}\right)\right] \left|\psi_{\mathrm{h}ij}(x)\right|^2. \tag{9}$$

where $\mathrm{m_{eD}}_i$ is effective mass of electron's state density with value $\mathrm{m_{eD1}} = 0.19\mathrm{m_0}$, $\mathrm{m_{eD2}} = 0.417\mathrm{m_0}$, and $\mathrm{m_{hD}}_i$ effective mass of hole's state density with value $\mathrm{m_{hD1}} = 0.645\mathrm{m_0}$, $\mathrm{m_{hD2}} = 0.251\mathrm{m_0}$, $\mathrm{m_{hD3}} = 0.29\mathrm{m_0}$. E_F is the Fermi energy which is set to $-\phi_B$.
The MOS gate capacitance C_g equals the series combination of the capacitances of C_{poly}, C_{sio_2} and C_{si} [1]:

$$\frac{1}{C_g} = \frac{1}{C_{poly}} + \frac{1}{C_{sio_2}} + \frac{1}{C_{si}} \tag{10}$$

where

$$\begin{cases} C_{poly} = \dfrac{\mathrm{d}Q_{poly}}{\mathrm{d}U_{poly}} \\ C_{sio_2} = \dfrac{\varepsilon_{\mathrm{ox}}}{t_{sio_2}} \\ C_{si} = \dfrac{\mathrm{d}Q_{si}}{\mathrm{d}U_{si}}, \end{cases} \tag{11}$$

where Q_{poly} and Q_{si} are the electric charge, U_{poly},U_{si} is the potential drop of the Poly-Si layer and Si layer. The stationary capacitance is the ratio of the total charge to the total voltage. In our case the capacitance of MOS structure is a nonlinear function of voltage, so the definition of differential capacitance is the ratio of charge difference to potential difference.

We use eight parameters in our mathematical model to characterize the device, which will be extracted in our inverse method. The following is the standard values for the study.

- $p_1 : N_{0poly} = 1 \times 10^{21} cm^{-3}$
- $p_2 : \sigma_1 = 0.002\mu m$
- $p_3 : N_{const} = 0.1 \times 10^{17} cm^{-3}$
- $p_4 : N_{0si} = 5.0 \times 10^{17} cm^{-3}$
- $p_5 : x_0 = 0.0\mu m$
- $p_6 : \sigma_2 = 0.2\mu m$;
- $p_7 : t_{sio_2} = 2.5nm$
- $p_8 : V_{fb} = 0.15v$

N_{0poly}, σ_1 are the parameters in the doping profile $N_{poly}(x)$ of the Poly-Si layer, and N_{const}, N_{0si}, x_0, σ_2 are the parameters in the doping profile $N_{0si}(x)$ of the Si layer. t_{sio_2} is the thickness of the Oxide layer. V_{fb} is the flatten band potential.

3. Numerical Method and Model Analyzing

3.1. Solution of Poisson Equation

In this paper, finite element method is used to solve Poisson equation and it leads to a nonlinear system. Relaxation Newton method is applied to solve the nonlinear problem. For classical model, Newton iteration is:

$$[-\frac{\mathrm{d}}{\mathrm{d}x}\left(\varepsilon(x)\frac{\mathrm{d}}{\mathrm{d}x}\right) - \beta q(p^n(x) + n^n(x))](\Delta\phi) = \frac{\mathrm{d}}{\mathrm{d}x}\left(\varepsilon(x)\frac{\mathrm{d}\phi^{\mathrm{n}}(\mathrm{x})}{\mathrm{d}x}\right) + q(p^n(x) - n^n(x) + N_d(x)), \tag{12}$$

where $\beta = \dfrac{kT}{q}$. In quantum region, it is tedious to compute Jacobi matrix and classical form is taken as an approximation:

$$[-\frac{\mathrm{d}}{\mathrm{d}x}\left(\varepsilon(x)\frac{\mathrm{d}}{\mathrm{d}x}\right)-\beta q(p_{qm}^{n}(x)+n_{qm}^{n}(x))](\Delta\phi) = \frac{\mathrm{d}}{\mathrm{d}x}\left(\varepsilon(x)\frac{\mathrm{d}\phi^{\mathrm{n}}(\mathrm{x})}{\mathrm{d}x}\right)+q(p_{qm}^{n}(x)-n_{qm}^{n}(x)+N_d(x)). \tag{13}$$

The (n+1)th iteration is computed from the nth iteration using

$$\Phi^{n+1} = \Phi^{n} + \omega\Delta\Phi$$

$0 < \omega < 0.1$ is empirically chosen to speed up convergence.

3.2. Solution of Schrödinger Equation

Finite volume method is used for solving Schrödinger equation and leads to a formal algebra eigenvalue problem $A\Psi = E\Psi$. It is not necessary to compute all the eigenvalues, because charge density (8), (9) is exponentially dependent on the eigenvalues and only small eigenvalues are important. Small eigenvalues of the Hamiltonian are computed using sturm sequencing and bisection and the eigenvectors are found by performing inverse iteration.

3.3. CV Simulation Process

The calculation starts with an initial guess for the electrostatic potential $\phi(x)$ according to the gate bias V_g and the Schrödinger equation can be solved. Once the eigenenergies and the corresponding wave functions have been obtained, the charge density throughout the quantum region is calculated. The Poisson equation is solved to get the electrostatic potential. The whole process is repeated until the input and the output potential agree within preestablished convergence limits. After attaining the electrostatic potential distribution, electric charge Q_{poly} and Q_{si} can be computed by $Q_{poly(si)} = \int_{t_{poly}(t_{si})} \rho(\phi(x), x)dx$. At last, The gate capacitor V_g is calculated by (10) and (11). The whole process can be formulated by a general form :

$$C_g = F(V_g, \bar{P}), \tag{14}$$

where $\bar{P} = (p_1, p_2...)$ represents the considered parameters.

To make sure the solution precise, the quantum region is divided as finely as possible for semiclassical model. It leads to large computation if Poisson and Schrödinger equations are solved on the same mesh. It is improved by only solving Schrödinger equation on fine mesh. Poisson equation and Schrödinger equation exchange values of potential $\psi(x)$ and charge density $\rho(x)$ by interpolation. h_p, h_s denote the mesh size for Poisson equation and Schrödinger equation separately. In table 1, the L_2 norm of CV(40 points) relative error and CPU time are presented. It is easily seen that the interpolation method saves 10 seconds with small lost of accuracy. It

mesh size (nm)	$h_p = h_s = 0.1$	$h_p = 0.2, h_s = 0.1$	$h_p = h_s = 0.2$
relative error	0.002	0.0053	0.0094
CPU time (s)	50	40	25

Table 1: Relative error and CPU time on different mesh

is more important to save time for the inverse work, so interpolation method can make the inverse process efficient.

3.4. Model Analysis

CV curve is more easily measured with high frequency (HF) gate voltage than with low frequency gate voltage , so we are interested the CV curve of HF mode. Minority charge can not be detected, therefore hole density $p(x)$ for N-type Si is neglected. Based on experimental result, the quantum region of semiclassical model is set $L_q = 0.01\mu m$. Fig.2-7 are the CV curves of different scale models.

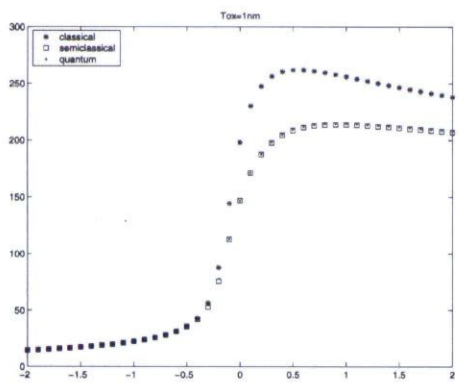

Figure 2: CV for different models, Tox=1nm.

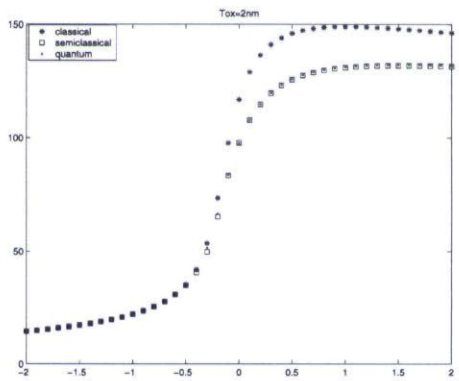

Figure 3: CV for different models,Tox=2nm

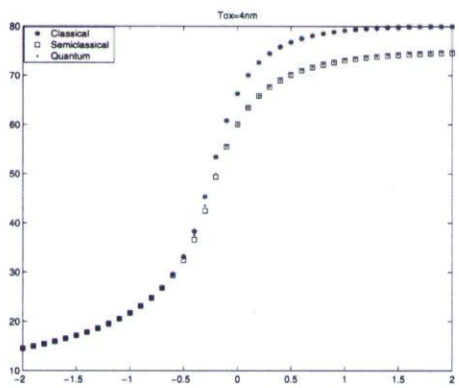

Figure 4: CV for different models, Tox=4nm.

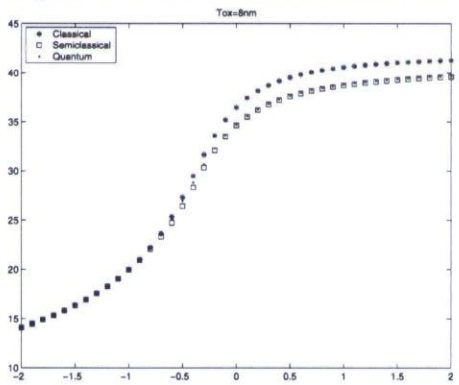

Figure 5: CV for different models,Tox=8nm

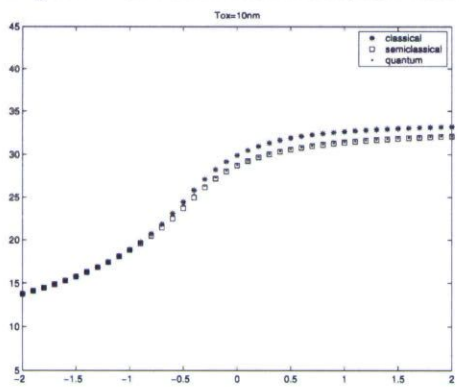

Figure 6: CV for different models,Tox=10nm

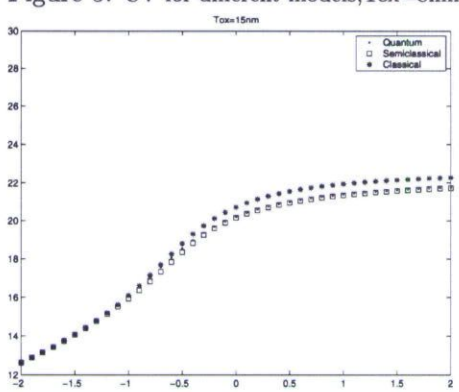

Figure 7: CV for different models,Tox=15nm

It is shown semiclassical model approximates quantum model perfectly. Semiclassical model

and quantum model are approaching classical model as oxide layer increases. To compute 40 CV points, semiclassical model consumes about 40 seconds while it takes quantum model nearly half hour. Semiclassical model not only saves the computing time greatly, but also includes QM effects correctly, so it is a good model to do the inverse work.

Apparently, large quantum region of semiclassical model decreases the difference of semiclassical model and quantum model at the cost of computing time. To compare the precision and CPU time of variant quantum region of semiclassical model, 40 points CV curve for different quantum region are computed and compared to quantum model. Fig. 8 shows L_2 norm of the relative error and CPU time. It is seen that the precision decrease slowly while the CPU time increases sharply when the quantum region is larger than $0.01\mu m$. So it is reasonable to set $L_q = 0.01\mu m$.

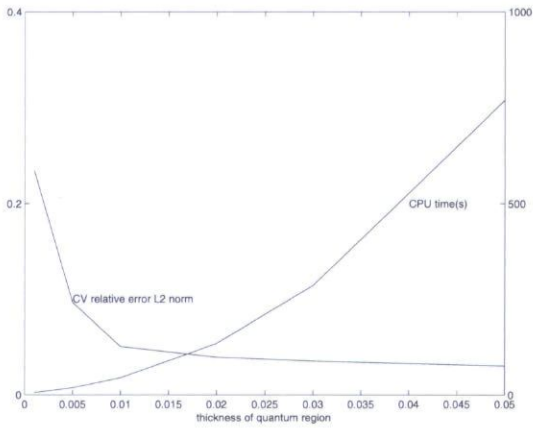

Figure 8: Relative error and CPU time of CV for different quantum region.Tox=1nm

4. Inverse Method and Results

Parameters are extracted by fitting CV curve. It will be useful for the inverse process to know the considered parameters' effects on CV curve. By observing the CV curves of each parameter when it deviates from the standard value, the 3rd is the least sensitive to the CV curve while the 7th is the most sensitive one. The scales of the parameters are greatly different. In order to compare their effects on CV curve in the same scale, we normalize them by setting the standard values as the base and the multiplying coefficients as the new parameters. To describe parameters' effects on CV curve by quantity, sensitivity of the parameter is defined as following:

$$S_i = \sqrt{\sum_{j=1}^{41} [\frac{F(Vg_j, \bar{P}_i) - F(Vg_j, \bar{P})}{0.01}]^2},$$

where $Vg_j = -2.0 + j \times 0.1$, $\bar{P}_i$ denotes the ith parameter deviates 1% from the standard value while others fixed at the standard values. Let

$$a_{ij} = [\frac{F(Vg_j, \bar{P}_i) - F(Vg_j, \bar{P})}{0.01}],$$

where $A = (a_{ij})_{8\times 41}$, $M = AA'$ and A' is the transfer matrix of A. Condition number of matrix M reflects the property of the inverse problem. Here the condition number (CN) of M and sensitivity of the parameters are presented in Table 2: It is obvious that $P_3(N_{const})$ is the least

S_1	S_2	S_3	S_4	S_5
0.1548	0.1355	0.0106	0.5065	0.9910
S_6	S_7	S_8		CN
0.0467	3.8880	0.4066		1.8717×10^{12}

Table 2: Parameter sensitivities in semiclassical model of HF mode

sensitive parameter. It may cause much trouble in inverse process. CN of HF model reaches 10^{12} which may cause much difficulty to extract the parameters simultaneously. Some technique is needed to do the inverse work.

For a group $\{C_{g_i}\}_{i=1}^n$ measured at $\{V_{g_i}\}_{i=1}^n$ correspondingly, the inverse problem is to confirm $\bar{P}$ which minimize the difference of $\{C_{g_i}\}_{i=1}^n$ to $\{F(V_{g_i}, \bar{P})\}_{i=1}^n$ at some sense. It is convenient to use L_2 norm for the fitting problem. If the Newton method is used to solve the least square problem directly, the large condition number 10^{12} of Jacobi matrix undoubtedly makes the inverse problem ill-conditioned. Here we implement the Levenberg-Marquardt (LM) optimization method to overcome this trouble. The object function is:

$$G(\bar{P}) = \sum_{i=1}^{n} [\frac{C_{g_i} - F(V_{g_i}, \bar{P})}{C_{g_i}}]^2 + \beta ||\bar{P}||^2.$$

Newton method is used to determine $\bar{P}$ to minimize $G(\bar{P})$ as $\beta \to 0$. The total error is set to be :

$$E(\bar{P}) = \sum_{i=1}^{n} [\frac{C_{g_i} - F(V_{g_i}, \bar{P})}{C_{g_i}}]^2.$$

Table 3 gives the considered parameters' standard values as the exact values and deviate up 10% as the initial values for numerical simulation. In Table 4, the inverse results are presented when parameters are extracted simultaneously.

parameter	P_1	P_2	P_3	P_4
exact value	1.0	0.002	0.1	5.0
initial value	1.1	0.0022	0.11	5.5
parameter	P_5	P_6	P_7	P_8
exact value	0.0	0.1	0.0025	0.15
initial value	0.1	0.11	0.00275	0.0165

Table 3: The standard values and the initial values

The inverse results verify the correctness of the prediction by the CN analysis. The 3rd parameter N_{const} can not come back to its standard value. We should add some technique to the inverse process. From the sensitivity analysis, the 3rd parameter is the least sensitive one. Our idea is to freeze the 3rd one firstly. After extracting the other parameters to some extent, put the 3rd into the inverse process. This method improves the precision of the inverse result greatly. In table 5, the inverse results with this technique are presented.

parameter	P_1	P_2	P_3	P_4
inverse value	0.99811438	0.00199548	0.14281769	4.95687738
relative error	0.00188562	0.00226	0.4281769	0.00862456
parameter	P_5	P_6	P_7	P_8
inverse value	0.00005649	0.09944950	0.00250001	0.14999929
relative error	0.00005649	0.005505	0.000004	0.000007

Table 4: Inverse results for semiclassical model of HF mode

parameter	P_1	P_2	P_3	P_4
inverse value	1.00025734	0.00200062	0.10855365	4.99036102
relative error	0.00025734	0.00031	0.0855365	0.0019278
parameter	P_5	P_6	P_7	P_8
inverse value	0.00001437	0.09987529	0.0025000	0.14999860
relative error	0.00001437	0.0012471	0.000000	0.000009

Table 5: Inverse results with order technique

We did a lot of inverse experiments with different initial cases. If the initial values deviate not more than 20%, the inverse result is satisfied. It is acceptable for practical device design.

5. Conclusion

This paper mainly analyzes different scale models of 1-D MOS capacitor. Numerical results show that semiclassical model includes QM effect as exactly as quantum model. Semiclassical model is not time-consuming, so it is a good choice to do parameters extraction for ultrathin oxide device. With semiclassical model, the parameters' effects to the CV curve is firstly considered. It is very helpful for us to propose an efficient inverse strategy. When the initial values offset is less than 20%, our strategy can give good inverse results. By a measured CV curve, we can use simplified model to give a guess value for sensitive parameters which differs not more than 20% from the exact value. So our strategy is applicable for practical problem.

As the thickness of the oxide layer decreases to sub-2.0nm, the tunnelling current increases in a nearly exponential manner. This increase in current adversely affects the MOS device performance [3, 10]. Thus, it is important to predict the tunnelling current for the development of advanced MOS device. The device decreases equally in each dimension, 2-D model must be considered for smaller dimension device. We will consider these in future work.

Acknowledgement. The authors are very grateful to Professors Wei Cai and Xiaoyang Liu for their helpful discussions.

References

[1] N. Arora, MOSFET models for VLSI circuit simulation, theory and practice, Wien: Springer–Verlag, 1993.

[2] Technology roadmap for semiconductors, Semiconductor Industry Assoc., Austin, Tx, 1997.

[3] Chang-Hoon Choi, Jung-Suk Goo, Tae-Young Oh and Zhiping Yu, MOS C-V characterization of ultrathin gate oxide thickness (1.3-1.8nm), *IEEE Electron Device Letters*, **20** (1999), 292-294.

[4] J.H. Davies, The physics of low-dimensional semiconductors, an introduction, Cambridge University Press Oxford, 1998.

[5] S.A. Harelard, S. Jallepalli and G. Chindalore, A simple model for quantum mechanical effects in hole inversion layers in silicon PMOS device, *IEEE Transactions on electron device*, **44** (1997), 1172-1173.

[6] K. Iniewski and C.A.T. Salama , A new approach to CV profiling with sub-Debye-length resolution, *Solid-st. Electron*, **34** (1991), 309-314.

[7] F. Rana, S. Tiwari and D.A. Buchanan, Self-consistent modeling of accumulation layers and tunnelling currents through very thin oxides, *Appl. Phys. Lett.*, **69** (1996), 1104-1106.

[8] Qiqing Shu, Theory of electron tunelling, Senscice Publisher, 1998.

[9] J. Suñé, P. Olivo and B. Rccó, Self-consistent solution of the Poisson and Schrdinger equations in accumulated semiconductor-insulator interfaces, *J. Appl. Phys.*, **70** (1991), 337-345.

[10] Nian Yang, W.K. Henson, and J. R. Hauser, Modeling study of ultrathin gate tunnelling current and capacitance-voltage measurments in MOS device, *IEEE Transactions on electron Device*, **46** (1979), 1464-1471.

[11] T. Yu and W. Cai, FIFA Fast interpolation and filtering algorithm for calculating dyadic Green's function in the electromagnetic scattering of multi-layered structures, *Commun. Comput. Phys.*, **1** (2006), 229-260.

[12] Pingwen Zhang, Yi Sun, Haiyan Jiang and Wei Yao, Multi-scale methods for inverse modeling in 1-D MOS capacitor, *Journal of Computational Mathematics*, **21** (2003), 85-100.